Available online at www.sciencedirect.com

ScienceDirect

Physics Procedia 10 (2010) 111–116

Physics Procedia

www.elsevier.com/locate/procedia

3rd International Symposium on Shape Memory Materials for Smart Systems

Role of Si in improving the shape recovery of FeMnSiCrNi shape memory alloys

Bikas C. Maji* and Madangopal Krishnan

Materials Science Division, Bhabha Atomic Research Centre, Mumbai – 400 085, INDIA

Abstract

The effect of Si addition on the microstructure and shape recovery of FeMnSiCrNi shape memory alloys has been studied. The microstructure of these alloys remains single-phase austenite (γ) up to 6% Si addition and beyond that it becomes two-phase γ+δ-ferrite. The Fe5Ni3Si2 type intermetallic phase starts appearing into the microstructure after 7% Si and makes these alloys brittle. The amount of shape recovery increases monotonically till 6% Si addition and is proportional to the amount of stress induced ε martensite. Alloys containing >6% and <4% Si show poor recovery due to formation of δ-ferrite and stress induced α' martensite respectively. Si addition decreases the stacking fault energy (SFE) of the γ phase and resulted in easier nucleation of stress induced ε martensite. The amount of athermal ε martensite decreases with increase in Si.

Keywords: Fe-based shape memory alloy; alloying; martensite; shape recovery; stacking fault energy

1. Introduction

The shape memory effect (SME) associated with the γ (fcc) - ε (hcp) martensite transformation was first reported by Enami et al. [1] in Fe-18.5% Mn alloy (the amount of shape recovery was less than 10 %!). Subsequently, Sato et al. [2] showed (in single crystals) that the addition of 1% Si to Fe-30Mn single alloy could significantly improve its shape recovery. Murakami et al. [3] were the first to developed polycrystalline Fe-Mn-Si alloys, but these only showed a little more than 1.7% recovery. However, these researchers could later show that the extent of shape recovery increases with Si content up to 6.5%. According to Sato et al. [4] and Murakami et al. [5], the beneficial effect of Si addition on the shape recovery of Fe-Mn alloys could be attributed to three major factors: i) lowering of the Neel transformation temperature (T_N) of γ phase below the γ to ε martensite start transformation temperature (M_S) without affecting the M_S temperature itself; ii) improvement in strength of the austenite matrix and iii) lowering of the SFE of γ phase. Murakami et al. [5] also claimed that the relative position of the M_S and T_N temperature is very important: the stress induced transformation will not take place and no shape recovery can be achieved when T_N lies above M_S. However, Andersson et al. [6] have shown that it is possible to form a large

* Corresponding author. Tel.: +91-22-2559 0469; fax: +91-22-2550 5151.
E-mail address: bikchan@barc.gov.in.

1875-3892
doi:10.1016/j.phpro.2010.11.084

amount of martensite even when the $M_S < T_N$. Gulyaev [7] have also reported that addition of Si significantly enhances the yield strength from 180 MPa in Fe-30Mn alloy to 350MPa in Fe-30Mn-5.5Si alloy. On the other hand, Tsuzaki et al. [8] and Tomota et al. [9] studied the effect of thermal cycling between M_f and A_f in Fe-15.5 Mn, Fe-24.4Mn, Fe-15.5Mn-6Si and Fe-24.5Mn-6Si (mass%) alloys and contend that Si causes the improvement in shape recovery by making the movement of partial dislocations reversible and restricting permanent slip in γ phase. In another study, Gavriljuk et al. [10] reported that Si increases the concentration of free electrons promotes the tendency for short range ordering, which could assist in improvement of shape recovery.

These studies only show that, so far, the exact role Si plays for enhancing the shape recovery is not clear, particularly in the case of Fe-Mn-Si-Cr-Ni alloys, where T_N lies below M_s (due to addition of Cr and the lower amount of Mn [11]). In addition, in these alloys the amount of Si was always maintained ~5-6%, which is less than the minimum required to attain maximum recovery. The present study is attempt to determine the exact role of Si in improving the shape recovery in Fe-Mn-Si-Cr-Ni based shape memory alloys by characterizing their microstructure, shape recovery and mechanical properties.

2. Experimental

The nominal compositions of the alloys used in the present work are given in Table 1. Alloy buttons were prepared by non-consumable vacuum arc melting under argon atmosphere using high purity (99.95%) Fe, Mn, Si, Cr and Ni. Arc melted buttons (Alloys 1 to 7) were hot rolled at 925^{o}C into strips of 0.5 mm thickness. These were then solution treated for 1 h at 1000^{o}C. As Alloys 8 and 10 were difficult to roll and developed cracks, specimens from these were cut directly from the arc melted buttons and then solution treated for 6 h at 1000^{o}C.

Optical microscopy, Scanning electron microscopy (SEM) and X-ray diffraction (XRD) were employed for microstructural characterization. XRD analysis was carried out using Mo-kα radiation ($\lambda_{k\alpha 1}$= 0.7093Å). The chemical compositions of constituent phases were measured by electron probe micro analysis (EPMA). The forward and reverse martensite transformation temperatures were determined on a differential scanning calorimeter (DSC) at a heating/cooling rate of 10^{o}C/min. The shape recovery of these alloys was evaluated using a simple bend test. The amount of recovery was determined by applying a pre-strain between 2-8% followed by recovery annealing at 600^{o}C for 10mins. Tensile tests of flat tensile specimens of 12.5 mm gauge length were performed at room temperature and a strain rate of 6.7×10^{-4}.

3. Results and Discussion

3.1 Microstructure

Figure 1 shows a few representative optical micrographs of Alloys1 to 10 that were solution heat treatment at 1000^{o}C. These micrographs show that up to 6% Si the microstructure is essentially single phase austenite (γ) with some amount of ε martensite. The same can also be obtained from the XRD patterns presented in Fig.2a. Further analysis reveals that the amount of martensite decreases with increasing Si content. As revealed by the XRD pattern, Alloy 7 containing 7% Si shows a two-phase microstructure (Fig. 1b) consisting of γ (appears light in contrast) and ~45% blocky δ-ferrite phase (appears dark). The composition analysis by EPMA, given in Table 2, shows that the matrix γ phase is richer in Ni and Mn and depleted in Cr and Si. In a complementary manner, δ-ferrite phase is

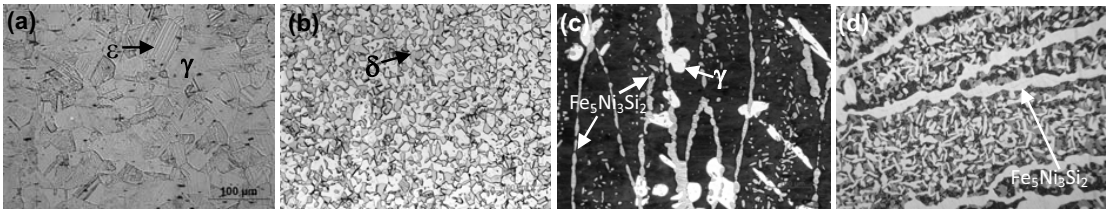

Fig. 1: Optical micrographs showing microstructures consists of (a) single phase γ in Alloy6, (b) two phase γ + δ-ferrite in Alloy7 (c) δ-ferrite + γ + $Fe_5Ni_3Si_2$ intermetallic phase in Alloy8 and (d) δ-ferrite + $Fe_5Ni_3Si_2$ type intermetallic in Alloy10.

richer in Cr and Si and leaner in Ni and Mn. These differences are expected as Ni and Mn are well known γ stabilizers, while Cr and Si are ferrite stabilizers [12].

The microstructure of Alloy8 (Fig. 1c) indicates the presence of three phases. Analysis of the XRD pattern shows that the microstructure is composed of γ (weaker reflections), δ-ferrite (stronger reflections) and an intermetallic phase. Thus, the matrix of Fig.1c is δ-ferrite and large bright grains adjacent to the grain boundaries are γ. As expected the composition analysis by EPMA, Table 2, showed that, in contrast to the composition of the large bright grains, the matrix is richer in Cr and Si and leaner in Ni and Mn. The intermetallic phase was identified to be with lattice parameter of 6.137Å and space group $P2_13$. So far no X-ray crystallographic data of this phase is available in literature. The only data available is of the π-phase ($Cr_3Ni_5Si_2$), which is iso-structural with this phase [13,14]. If we assume that Ni site is shared by Ni, Mn and Cr atoms, then the composition is very close to the stoichiometric $Fe_5Ni_3Si_2$, i.e. (Cr+Ni+Mn) is 32.55 at%, Si 19.29 at% and Fe 48.16 at%. This intermetallic phase is most likely the reason behind the brittleness in this alloy. Further increase in Si amount to 10% (Fig.1d) only resulted in a higher amount of $Fe_5Ni_3Si_2$ phase and absence of the grain boundary γ phase.

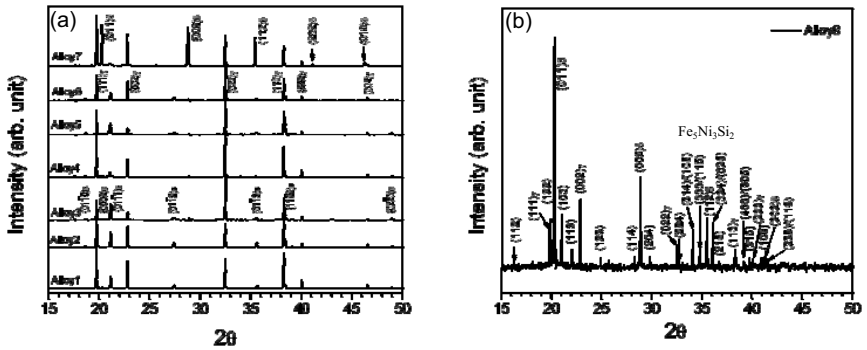

Fig. 2: XRD patterns of solutionized specimens (a) Alloy1 to Alloy7 and (b) Alloy 8 showing the major phase constituents.

The above observations show that the stability of the γ phase reduces with Si content, as observed by the occurrence of a two-phase microstructure when Si is 7%, and is further diminished by the appearance of the $Fe_5Ni_3Si_2$ phase, when Si is higher than 7%. When the Si content reaches 10%, γ phase is totally absent in the microstructure.

Table 1: Nominal alloy compositions

Alloy	Nominal compositions *(wt %)*				
	Mn	Cr	Ni	Si	Fe
Alloy1	14	9	5	1	Balance
Alloy2	14	9	5	2	Balance
Alloy3	14	9	5	3	Balance
Alloy4	14	9	5	4	Balance
Alloy5	14	9	5	5	Balance
Alloy6	14	9	5	6	Balance
Alloy7	14	9	5	7	Balance
Alloy8	14	9	5	8	Balance
Alloy10	14	9	5	10	Balance

Table 2: Chemical composition of phases

Alloy	Phase	Compositions *(wt %)*			
		Cr	Ni	Mn	Si
Alloy7	γ	8.993	5.018	14.695	7.333
	δ	10.278	4.425	13.372	8.480
Alloy8	δ	9.442	4.590	13.711	9.561
	γ	8.290	5.288	15.407	7.839
	$Fe_5Ni_3Si_2$	9.816	7.840	17.940	10.802

3.2 Transformation temperatures

The transformation temperatures for the γ austenite to ε martensite transformation during cooling and those of the reverse transformation during heating were measured using small specimens of 40-50 mg weight in the temperature

range of -75°C to 200°C. The results obtained from these measurements, Fig. 3, clearly show that Si addition up to 6% does not significantly change the M_s of the γ to ε transformation; however, there is a slight increase in ε to γ transformation start temperature (A_s). The M_s and A_s temperatures drop above 6% Si, with alloys containing more than 7% Si not showing the martensitic transformation. Interestingly, the enthalpy of the γ–ε transformation decreases with increase in Si content. This corresponds to the athermal ε martensite amount decreasing with Si content and is substantiated by the metallographic and XRD observations.

3.3 Shape Recovery

Figure 4 presents the variation of shape recovery in Alloys 1 to 7, at different amounts of pre-strain. This plot essentially shows that the amount of shape recovery increases up to 6% Si amount. A detailed analysis reveals that, based on their shape recovery response, these alloys can be divided into two classes. Alloys containing up to 3% Si (Alloy1 to Alloy3) show poor shape recovery (<60% at 4% pre-strain) and alloys having Si 3-6% (Alloy4 to Alloy6) show good shape recovery (>60% at 4% pre-strain). The highest amount of shape recovery was observed in the case of Alloy6 and beyond that the recovery reduces. The low amount of shape recovery in the case of Alloy7 can be easily correlated to its microstructure, which contains ~45% δ-ferrite. It is obvious that in such microstructures less amount of stress induced martensite will form and shape recovery will be hindered.

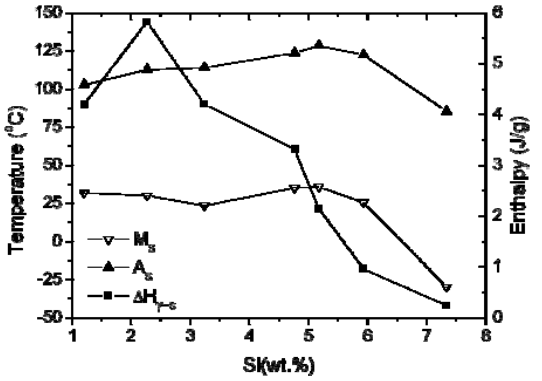

Fig. 3: Change in transformation temperatures and enthalpy of transformation due to Si addition.

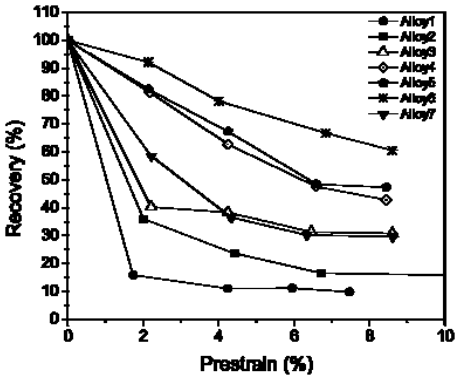

Fig. 4: Improvement in shape recovery due to Si

3.4 Mechanical properties

Figure 5a presents the room temperature tensile properties of Alloys 1 to 7. It is observed that the yield strength (0.2% proof stress) do not change substantially, at least up to 6% Si. This indicates that there is no significant increase in strength of γ matrix due to Si addition. The highest yield strength and lowest ductility was obtained in the case of Alloy7, which is possibly due to the high fraction of δ-ferrite in the microstructure. . The fractograph of Alloy7, Fig.5b, shows a typical cleavage type fracture, indicating the brittle nature of the fracture. Some cracks could also be noticed in this specimen, which possibly occur at the interface of γ and δ-ferrite due to the difference in extents of deformation suffered by these phases. The yield strength of Alloy3 is the lowest among the single-phase austenitic alloys, which may be on account of the higher amount of ε martensite in the microstructure. A slight increase in yield strength of Alloy5 could be due to its smaller grain size, as noted in optical microscopy.

3.5 Microstructural changes after pre-straining

Tensile specimens (solutionized at 1000°C) were pre-strained at room temperature up to 5% and examined for the microstructural changes within the gauge length. Quantitative Rietveld analysis [15] of the X-ray diffraction patterns from gauge portions was performed to determine the phase fractions. The amount of ε martensite present in the microstructure, before (solutionized state) and after straining, is presented in Fig.6a. It is clearly seen that the volume fraction of athermal ε martensite (V_{ath}) reduces with increasing Si amount. It can also be seen that the total amount of ε martensite (V_{tot}) formed during straining to 5% remains more or less same in all alloys but Alloy1. On

the other hand, the amount of stress induced ε martensite, (V_{tot} -V_{ath}), is found to increase with Si. However, the amount of stress induced ε martensite is low till 3% Si, after which it steadily increases upto 6% Si. These results

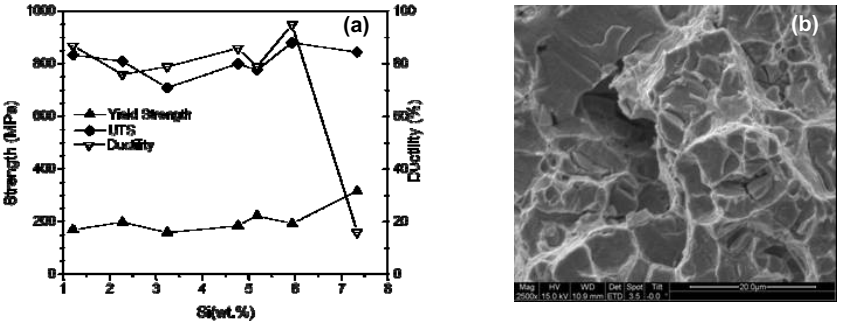

Fig.5: (a) Variation in mechanical properties due to Si addition and (b) the fracture surface of Alloy7 showing cleavage fracture.

show that with increasing Si content recovery increases, athermal martensite decreases and stress induced martensite increases. Thus, it is seen that shape recovery is proportional to the amount of stress induced ε martensite.

Another important result obtained from the X-ray diffractograms, Fig.6b, is that α' martensite forms during pre-straining in alloys with Si less than 4%. Metallographic examination of these samples showed the presence of α' martensite within bands of ε martensite (suggesting that α' is generated by the ε–α'transformation). Beyond 3% Si, only stress induced ε martensite is observed (the amount of α' martensite formed, if at all, is less than the detectable limit of powder X-ray diffraction). Thus, it is seen that the poor shape recovery of alloys with less than 4% Si is associated with formation of stress induced α' martensite.

The formation of stress induced ε martensite may be related to the SFE in these alloys. The probability of stacking fault determined by Warren-Averbach technique of X-ray line profile analysis [16], from which the SFE was derived using the relationship proposed by Schramm and Reed [17]. Figure 7 shows the SFE decreases with amount of Si. Therefore, it appears that ε martensite is more easily stress induced with a decrease in SFE. In this context, it is a surprise that the amount of athermal ε martensite decreases with Si addition when it should also have increased. This apparent contradiction points to a possibility that nucleation of ε martensite is affected by Si content. However, this can be resolved if it is likely that, Si addition, in some way, reduces the number of potent nuclei of ε martensite. The occurrence of stress induced martensite may then be related to the generation of nuclei by concomitant plastic deformation present during straining of austenite, i.e the yield stress may be close to the critical stress to induce martensite.

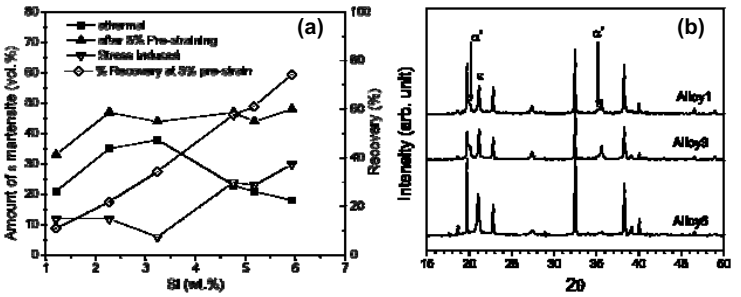

Fig. 6(a) Change in amount of athermal and stress induced ε martensite due to Si addition and its consequence on the shape recovery and (b) XRD patterns showing stress induce α' martensite.

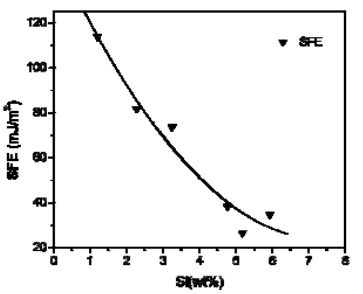

Fig. 7: Change in stacking fault energy (SFE) due to Si addition.

This study has shown that at least 4% Si is required for avoiding stress induced ε–α' transformation and addition of more than 6% is not possible due to the formation of δ ferrite. This study has also revealed that Si does not affect

the transformation temperature and the mechanical properties of austenite, though it reduces the formation of athermal martensite and as also the SFE. On the other hand, this study has shown that good shape recovery is observed when the transformation temperature is close to the ambient, when there is only little pre-existing athermal martensite, when the SFE is low and when the yield stress of the matrix is close to the critical stress to induce martensite. It is in this context that role of Si in improving the memory becomes apparent.

4. Conclusions

The important results obtained from this study can be summarized as follows:

i. In FeMnSiCrNi alloys, single phase γ microstructure is stable only up to 6% Si. Alloys having more than 6% Si show a microstructure composed of γ + δ-ferrite phases. $Fe_5Ni_3Si_2$ type intermetallic phase starts appearing in the microstructure above 7% Si and causes these alloys to be brittle.

ii. The shape memory effect in these alloys is essentially due to stress induced ε martensite and the extent of shape recovery is proportional to the amount of stress induced ε martensite formed during pre-straining. The observation of poor shape recovery in alloys with Si <4% and >6% is due to the formation of stress induced α' martensite and δ-ferrite, respectively.

iii. Si reduces the SFE in these alloys enhances the nucleation of stress induced martensite and consequently the amount of shape recovery.

iv. Si decreases the amount of athermal ε martensite, probably through a reduction in the population of potent nuclei.

References

1. K. Enami, A. Nagasawa and S. Nenno, 1975, *Scr. Metall.*, 9, 941.
2. A. Sato, E. Chisima, K. Soma and T. Mori, 1982, *Acta Metall*., 30, 1177.
3. M. Murakami, H. Otsuka, H. Suzuki and S. Matsuda, 1987, *Trans. ISIJ*, 27, 88.
4. A. Sato, Y. Yamaji and T. Mori, 1986, *Acta Metall*., 34, 287.
5. M. Murakami, H. Otsuka, H. Suzuki and S. Matsuda, 1986, in *Proceedings of International Conference on Martensitic Transformations (ICOMAT-86), Nara, Japan*, 985.
6. M. Andersson, R. Stalmans and J. Agren, 1998, *Acta Metall*., 46, 3883.
7. A.A. Gulyaev, 1995, *J. Phys.IV*, 5, 469.
8. K. Tsuzaki, M. Ikegami, Y. Tomota, K. Kurokawa, W. Nakagawara and T. Maki, 1992, *Mater. Trans. JIM*, 33, 236.
9. Y. Tamota, M. Piao, T. Hasunuma and Y. Kimura, 1990, *Japan Inst. Metals*, 54, 628.
10. V.G. Gavriljuk, V.V. Bliznuk, B.D. Shanina and S.P. Kolesnik, 2005, *Mat. Sci. Engg. A*, 406, 1.
11. H. Otsuka, H. Yamada, T. Maruyama, H. Tanahashi, S. Matsuda and M. Murakami, 1990, *ISIJ Inter.,* 30, 674.
12. F.B. Pickering, 1978, *Physical Metallurgy and the Design of Steels*, Applied Science Publishers Ltd., London, 226.
13. E.I. Gladyshevskii, P.I. Kripyakevich and Yu.B. Kuz'ma, 1962, *J. Str. Chem.,* 3, 402.
14. B.C. Maji, M. Krishnan and V.V. Rama Rao, 2003, *Metall. Trans A*, 34A, 1029.
15. H.M. Rietveld, 1967, *Acta. Cryst.,* 22, 151.
16. B.E. Warren and B.L. Averbach, 1950, *J. Appl. Phys*., 21, 595.
17. Schramm and R.P. Reed, 1975, *Met. Trans. A*, 6A, 1345.